

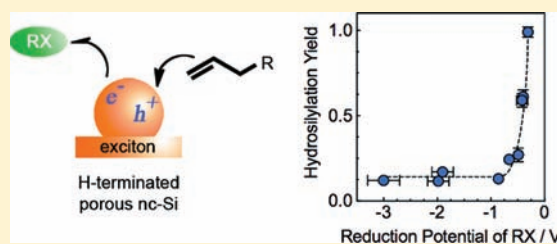
# Toward a Mechanistic Understanding of Exciton-Mediated Hydrosilylation on Nanocrystalline Silicon

Lawrence A. Huck\* and Jillian M. Buriak\*

Department of Chemistry, University of Alberta, 11227 Saskatchewan Drive, Edmonton, Alberta T6G 2G2, and National Research Council Canada, National Institute for Nanotechnology, 11421 Saskatchewan Drive, Edmonton, Alberta T6G 2M9, Canada.

Supporting Information

**ABSTRACT:** White-light initiated hydrosilylation of nanocrystalline porous silicon was found to be far more efficient (in terms of both kinetics and yield) in the presence of electron-accepting molecules with suitably high reduction potentials, particularly halocarbons. It is known that absorption of visible light by nanocrystalline silicon results in the formation of excitons (electron/hole pairs) and that this exciton can be harnessed to drive a hydrosilylation reaction with an alkene; the Si–C bond forms as a result of attack of the  $\pi$ -electrons of the alkene on the positively charged holes. In order to better understand the white-light initiated mechanism through which this reaction takes place, and to compare with UV-mediated photoemission on Si(111)–H, a series of electron acceptors were screened for their effect on surface alkene hydrosilylation. A very strong correlation between reduction potentials ( $E_{\text{red}}$ ) of the oxidant and reaction efficiency was observed, with a minimum “turn-on”  $E_{\text{red}}$  required for an increase to take place. The oxidant appears to accept, or remove, the electron from the nanocrystallite-bound exciton, favoring attack by the alkene on the positively charged Si nanocrystallite, leading to Si–C bond formation. Radical reactions were discounted for a number of reasons, including lack of effect of radical traps, no apparent Si–Cl bond formation, lack of oxidation of the surfaces, and others. Unlike with other oxidants such as nitro-aromatics, halocarbons do not cause additional surface reactions and promote very clean, fast, and selective hydrosilylation chemistry.



## INTRODUCTION

Functionalization of semiconductor surfaces to tailor the physical and chemical properties is an important goal of surface science because of the significance of these materials in the fabrication of electronics, sensors, and other devices.<sup>1</sup> Much attention in this regard has been directed toward Si–C bond formation on silicon surfaces [Si(100)–H<sub>x</sub>/Si(111)–H “flat silicon”<sup>1c,2,3</sup> and nanocrystalline/porous<sup>2a,p,4,5</sup>]. Hydrosilylation of hydrogen-terminated silicon is a common route to functionalization of the surface;<sup>2a–1,3–6</sup> irradiation with UV or visible light is a typical method of initiating this reaction and has been the subject of many mechanistic studies since the original report of these reactions on flat<sup>2c,7</sup> and nanocrystalline porous silicon<sup>4a</sup> (hereafter “PS”) in the 1990s. Figure 1 shows four proposed mechanisms for photoinitiated hydrosilylation: (i) Si–H bond homolysis, (ii) photoemission, (iii) plasmon-mediated, and (iv) exciton-mediated. For UV-initiated hydrosilylation, two mechanisms have been proposed: Si–H bond homolysis and subsequent radical-based hydrosilylation (Figure 1 i),<sup>2c</sup> and more recently, photoemission that generates positive charges on the surface (Figure 1 ii).<sup>3</sup> Visible-light initiation of hydrosilylation on flat silicon<sup>2f,6b,8</sup> and nanocrystalline silicon<sup>5</sup> is proposed to involve the formation of plasmons (Figure 1 iii) and quantum-confined excitons (localized electron [ $e^-$ ]/hole [ $h^+$ ] pairs; see Figure 1 iv), respectively. Visible light has insufficient energy to break the Si–H bond, and thus, homolytic cleavage of this bond is not implicated.<sup>2c</sup>

In each case, the next step in the reaction is attack of the positive charge on the surface by the alkene  $\pi$ -electrons to form the Si–C bond.<sup>9</sup> Visible-light initiated hydrosilylation on flat silicon is substantially slower than the visible-light initiated reaction on PS (several hours vs minutes).<sup>2f</sup> The present study investigates exciton-mediated hydrosilylation on PS (Figure 1 iv),<sup>5</sup> allowing a comparison with the nonexciton photoemission mechanism described by Hamers and co-workers for Si(111)–H (Figure 1 ii).<sup>3</sup> In each case, the presence of electron acceptors in proximity to the surface increases the efficiency of hydrosilylation; however, with PS, electron acceptors with much higher reduction potentials ( $E_{\text{red}}$ ) are required to remove the electron from the electron/hole pair, presumably because it is necessary to overcome the exciton binding energy.<sup>10</sup>

Since the first report on the properties of PS by Canham in 1990,<sup>11</sup> this form of hydrogen-terminated silicon continues to capture the attention of researchers attempting to take advantage of its porosity, high surface area, biocompatibility, and photoluminescence.<sup>12</sup> For example, PS has been studied for potential utilization in drug delivery,<sup>13</sup> various biological applications,<sup>14</sup> solar cells,<sup>14b,15</sup> and optical devices.<sup>16</sup> When PS is excited by a photon with an energy exceeding the band gap ( $\sim 1.8$  eV),<sup>17</sup> the resulting exciton is relatively long-lived due to quantum confinement

Received: September 12, 2011

Published: November 16, 2011

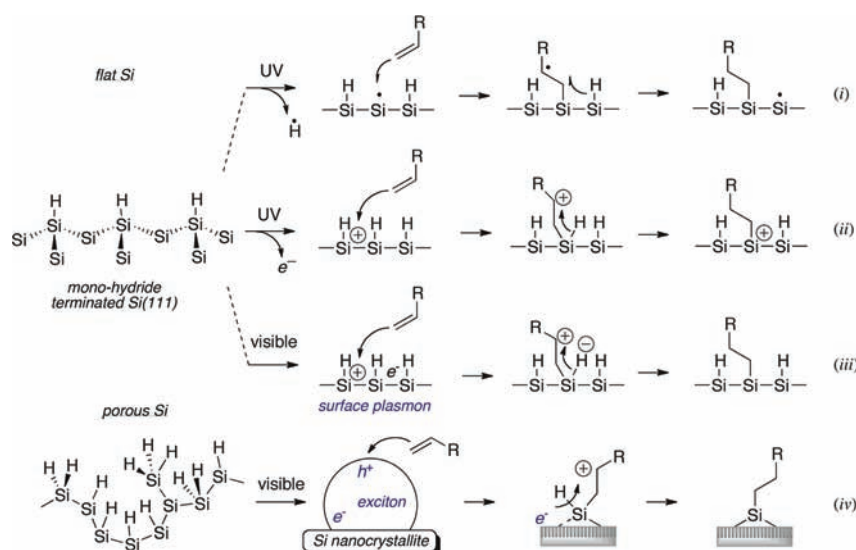


**Figure 1.** Four mechanisms previously proposed for the photoinitiated hydrosilylation on hydrogen-terminated silicon surfaces.

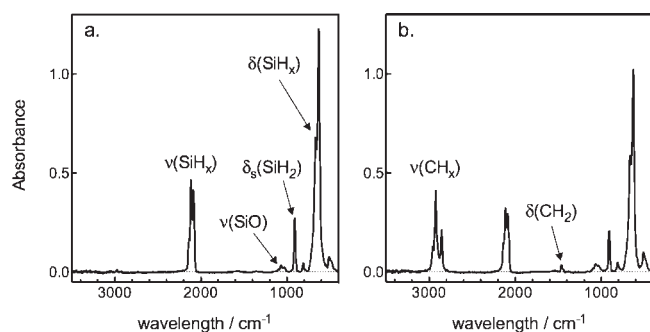


**Figure 2.** Transmission FTIR spectra of (a) freshly prepared porous silicon and (b) the same sample after undergoing exciton-mediated, white-light hydrosilylation with 1-dodecene. (Irradiation time 20 min,  $\sim 175 \text{ mW cm}^{-2}$ .)

effects, and one result of the recombination of the  $e^-/h^+$  pair is photoluminescence.<sup>18</sup> In addition to the technological applications, harnessing the exciton can be used to drive chemical reactions on PS including polymerization,<sup>19</sup> surface oxidation,<sup>20</sup> and hydrosilylation.<sup>5</sup> With respect to hydrosilylation, only photoluminescent PS was found to undergo efficient white-light mediated reaction pointing to the central role of the excitons in the chemistry.<sup>5</sup> The proposed exciton-mediated mechanism is shown in Figure 1 *iv*: upon excitation,  $h^+$  is attacked by the alkene  $\pi$ -electrons, which leads to Si–C bond formation. A hydride from the silicon is transferred to the resulting  $\beta$ -silyl cation, completing the reaction.

When carried out in an inert atmosphere, exciton-mediated hydrosilylation with 1-dodecene on PS results in reaction of  $13 \pm 5\%$  of the Si–H<sub>x</sub> bonds with minimal surface oxidation.<sup>5</sup> When the same reaction is carried out in air, the rate of hydrosilylation increases despite a substantial increase in surface oxidation.<sup>5</sup> As a good electron acceptor, O<sub>2</sub> may be accelerating the hydrosilylation reaction by trapping the electron of the exciton, leaving  $h^+$  more susceptible to nucleophilic attack by the alkene. Rehm et al. have shown that the photoluminescence of PS is quenched in the presence of molecules with suitable reduction potentials (nitro-substituted aromatics in their experiments), suggesting that electrons

can be extracted from the excitons of nanocrystalline silicon.<sup>18e</sup> Hamers and co-workers have shown that when electrons photoejected from Si(111)–H reduce a molecule with a high electron affinity in proximity to the surface, the yield of hydrosilylation increases (vide infra).<sup>3</sup> Presumably then, photohydrosilylation reactions on PS performed in the presence of a sacrificial oxidant should also result in a greater yield of hydrosilylation. Our experiments employed a series of oxidizing agents with a wide range of reduction potentials<sup>21</sup> as mediators to increase the rate and yield of hydrosilylation reactions on PS without a concomitant increase in surface oxidation.

## RESULTS AND DISCUSSION

Photoluminescent PS was formed via anodic etching of *n*-type silicon in 1:1:2 HF/H<sub>2</sub>O/EtOH with simultaneous white-light irradiation.<sup>5</sup> All photochemical reactions were performed in a nitrogen-filled glovebox. The hydrosilylation reaction was achieved by coating the sample with a small volume (40  $\mu\text{L}$ ) of the neat alkene or the alkene/oxidant mixture and irradiating the surface with white light from a standard halogen 300 W ELH projector bulb. Changes to the surface chemistry of PS can be monitored by transmission FTIR spectroscopy. Figure 2a shows a baseline corrected IR spectrum of freshly prepared PS, while Figure 2b shows the same sample after undergoing white-light hydrosilylation with 1-dodecene (hereafter “dodecene”) to full completion, which in this case is a reaction efficiency (%*E*, vide infra) of  $\sim 10\%$  of the Si–H<sub>x</sub> bonds. Two terms in the literature used to quantitate the amount of surface grafting are percent-efficiency<sup>4b</sup> (%*E*; eq 1) and the normalized CH<sub>x</sub> absorption<sup>2d</sup> ( $A_{\text{CH}_x, \text{norm}}$ ; eq 2). The percent efficiency estimates the number of SiH<sub>x</sub> bonds that have undergone hydrosilylation, assuming the SiH<sub>x</sub> absorption intensities do not change when adjacent to alkyl groups. The advantage of %*E* is that it is independent of the alkene/alkyne used,<sup>22</sup> but the disadvantage is that at very low conversions, the SiH<sub>x</sub> area changes very little; this problem is compounded by the broadening of the SiH<sub>x</sub> peak as the yield of hydrosilylation increases, coupled with the curved baseline typically associated with these PS samples. An accurate measurement is therefore difficult to obtain and typically we found the absolute

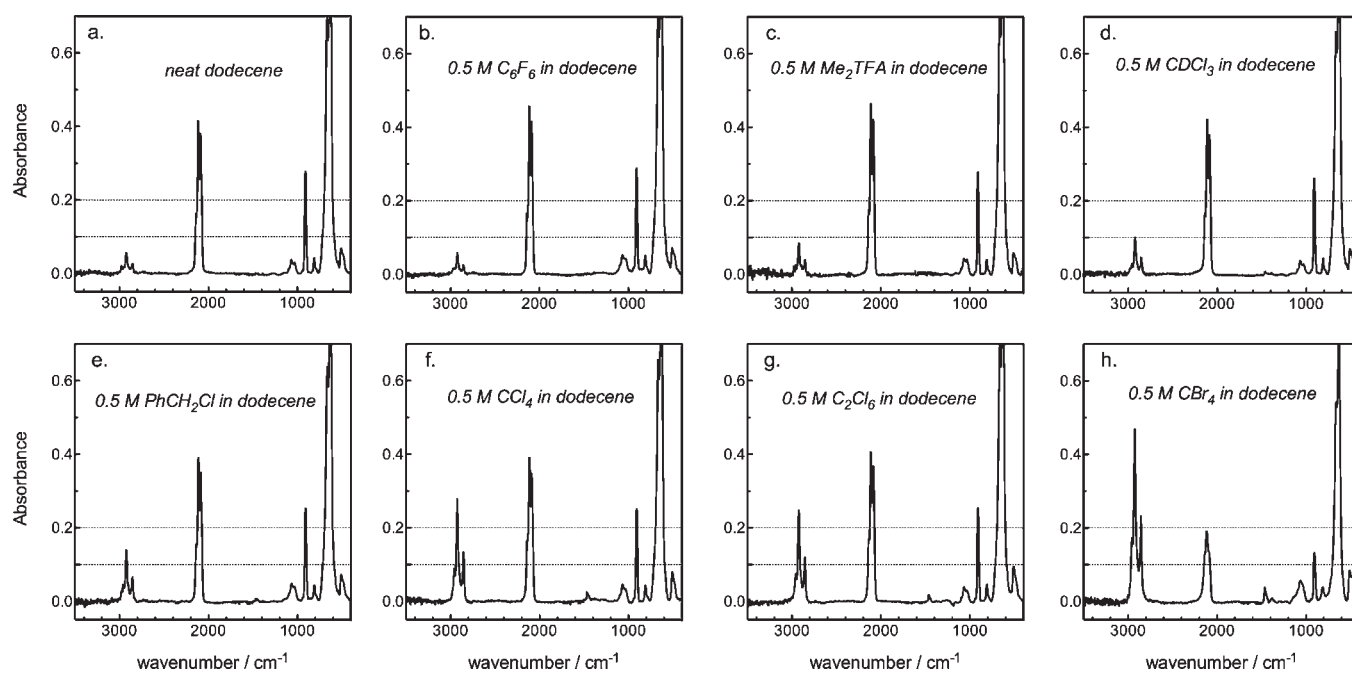


**Figure 3.** Transmission FTIR spectra of PS samples coated with (a) dodecene, (b–h) 0.5 M oxidizing agent in dodecene and exposed to white light ( $\sim 175 \text{ mW cm}^{-2}$ ) for 60 s.

error of this measurement to be  $\pm 3\text{--}5\%$ . With the normalized  $\text{CH}_x$  absorption, the focus is on a region that undergoes substantial change at low conversion, so obtaining accurate numbers is less of a concern; division of  $\Delta A_{\text{CH}}$  by  $A_{\text{SiH},0}$  accounts for the fact that not all samples have the same initial concentration of  $\text{SiH}_x$  bonds. Additional corrections would be necessary in order to compare different reactants (e.g., 1-hexene vs 1-octene).<sup>2d</sup> In our experiments, dodecene was chosen as our standard alkene and the hydrosilylation yields are reported using  $A_{\text{CH},\text{norm}}$  although %E is also given where appropriate.

$$\%E = \frac{(A_{\text{SiH},0} - A_{\text{SiH},t}) \cdot 100}{A_{\text{SiH},0}} = \frac{\Delta A_{\text{SiH}}}{A_{\text{SiH},0}} \quad (1)$$

$$A_{\text{CH},\text{norm}} = \frac{(A_{\text{CH},0} - A_{\text{CH},t})}{A_{\text{SiH},0}} = \frac{\Delta A_{\text{CH}}}{A_{\text{SiH},0}} \quad (2)$$

Dodecene solutions containing 0.5 M of an oxidizing agent (various halocarbons, two nitroaromatics, and *N,N*-dimethyltrifluoroacetamide [ $\text{Me}_2\text{TFA}$ ]) were prepared. PS samples were coated with a small volume of either neat dodecene or the dodecene/oxidizing agent solution and irradiated with visible light under identical conditions. Infrared spectra taken after *only* 60 s of white-light exposure to emphasize the differences in rate are shown in Figure 3, while the resulting yields and the reduction potentials of the oxidizing agents are given in Table 1. Compared to the yield of hydrosilylation observed with neat dodecene (Figure 3a), the presence of molecules with reduction potentials less than  $\sim -0.6 \text{ V}$  (vs SHE) do not bring about any significant change in the yield nor is any additional surface chemistry observed (for example, Figure 3b,c). In the presence of molecules with reduction potentials greater than  $-0.6 \text{ V}$ , however, there is a clear increase in the yield of hydrosilylation (Figure 3d–h).

The white-light hydrosilylation reaction on PS with alkenes and alkynes generally reaches its maximum yield within 20–30 min

**Table 1.** Hydrosilylation Yields ( $A_{\text{CH},\text{norm}}$ ) on Samples of Photoluminescent PS Hydrosilylation Coated with 0.5 M Oxidizing Agent in Dodecene and Exposed to White Light ( $\sim 175 \text{ mW cm}^{-2}$ ) for 60 s; Reduction Potentials ( $E_{\text{red}}$  vs SHE in Acetonitrile) of the Electron Acceptors Are also Given

oxidant	$A_{\text{CH},\text{norm}}^a$	yield (rel) <sup>b</sup>	$E_{\text{red}}/\text{V}^c$
none	$0.13 \pm 0.03$	1	$< -3^d$
$\text{C}_6\text{F}_6$	$0.12 \pm 0.02$	$0.9 \pm 0.2$	$-1.98^e$
$\text{Me}_2\text{TFA}$	$0.17 \pm 0.02$	$1.3 \pm 0.2$	$\sim -1.9^f$
4-nitrotoluene <sup>g</sup>	–	–	$-1.19^h$
$\text{CH}_2\text{Cl}_2$	$0.13 \pm 0.02$	$1.0 \pm 0.2$	$-0.86$
$\text{CDCl}_3$	$0.24 \pm 0.03$	$1.9 \pm 0.2$	$-0.66$
$\text{C}_6\text{H}_5\text{CH}_2\text{Cl}$	$0.27 \pm 0.04$	$2.1 \pm 0.3$	$-0.49$
$\text{C}_2\text{Cl}_6$	$0.59 \pm 0.04$	$4.5 \pm 0.3$	$-0.42^i$
trinitrobenzene <sup>g</sup>	–	–	$-0.41^j$
$\text{CCl}_4$	$0.61 \pm 0.02$	$4.7 \pm 0.2$	$-0.40$
$\text{CBr}_4$	$0.99 \pm 0.03$	$7.6 \pm 0.3$	$-0.24$

<sup>a</sup> Each yield is the average of 2–4 runs. <sup>b</sup> (Yield with 0.5 M oxidant)/(Yield with neat dodecene). <sup>c</sup> Unless otherwise stated, data from reference 24. <sup>d</sup> Reference 25. <sup>e</sup> Reference 26. <sup>f</sup> Estimated from the data in references 27 and 28. <sup>g</sup> The surface undergoes oxidation and other reactions. See text. <sup>h</sup> Reference 18e. <sup>i</sup> Estimated on the basis of the difference in the reduction potentials of  $\text{C}_2\text{Cl}_6$  and  $\text{CCl}_4$  in water given in reference 29. <sup>j</sup> Reference 30.

(e.g., Figure 2) with an efficiency of 10–20%.<sup>5</sup> In the present case, the highest yield was obtained in the presence of  $\text{CBr}_4$  ( $E \approx 55\text{--}60\%$ ; see Supporting Information, Figure S4), the halocarbon with the highest reduction potential of those studied; furthermore, the maximum conversion is achieved within 5–8 min. Because of the morphologically complex nature of PS relative to flat silicon, the maximum possible coverage on PS for alkyl groups may be slightly greater than the  $\sim 55\%$  maximum coverage for flat  $\text{Si}(111)\text{--H}$ .<sup>23</sup>

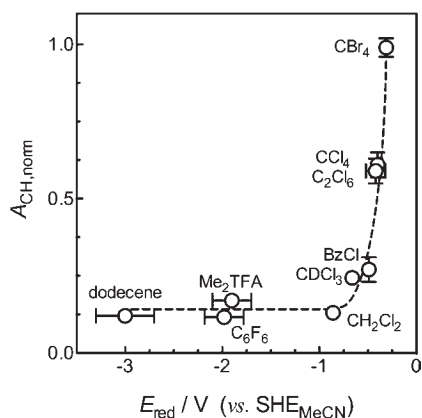


**Figure 4.** Yield of exciton-mediated hydrosilylation on PS after 60 s of photolysis plotted against the reduction potential of the halocarbon. The dashed line is an estimate of the trend.

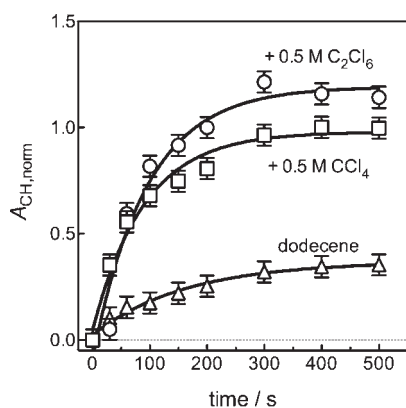


**Figure 5.** Plots of the growth of  $A_{\text{CH},\text{norm}}$  on PS coated with the dodecene solutions listed and exposed to white light ( $\sim 175 \text{ mW cm}^{-2}$ ). The solid lines are the fit of the data to eq 3.

To ensure that these reactivity differences could not be attributed to heat from the lamp, the light was passed through infra-red filters (see Experimental Section). The use of a 400-nm long-pass filter also ruled out any UV from the halogen lamp as the cause of the observed reactivity. The oxidizing agents employed do not absorb visible light (Supporting Information, Figure S3), and no hydrosilylation was observed when PS was coated with the dodecene/oxidizing agent mixtures and kept in the dark.

A correlation of the yield with the reduction potential of the oxidizing agent is observed (Figure 4). Once the reduction potential is more positive than  $\sim -0.6 \text{ V}$ , the yield of hydrosilylation increases rapidly. Except in the case of 4-nitrobenzene and 1,3,5-trinitrobenzene, the reaction is *not* accompanied by increased surface oxidation. Rehm et al. noted that nitroaromatics with reduction potentials more positive than  $\sim -0.9 \text{ V}$  are capable of quenching the PS photoluminescence and that the effectiveness of the quencher is positively correlated with the reduction potential of the quencher.<sup>18e</sup> A related study by Germanenko et al. using silicon nanocrystals reached similar conclusions.<sup>31</sup> In our experiments, irradiation of PS surfaces coated with dodecene containing nitro-substituted aromatics, particularly trinitrobenzene, results in increased surface oxidation, along with additional surface reactions. Reaction of the PS surfaces with nitroaromatics (both in the dark and upon photolysis) has been reported by

**Table 2.** Rate Coefficients ( $k_{\text{obs}}$ ) Calculated for the White-Light Initiated ( $\sim 175 \text{ mW cm}^{-2}$ ) Hydrosilylation Reaction of Dodecene on Photoluminescent PS at  $\sim 25 \text{ }^\circ\text{C}$ <sup>a</sup>

oxidant	$k_{\text{obs}}/10^{-3} \text{ s}^{-1}$
none (1-dodecene)	$6 \pm 1$
0.5 M $\text{CCl}_4$ in dodecene	$10 \pm 2$
0.5 M $\text{C}_2\text{Cl}_6$ in dodecene	$11 \pm 2$

<sup>a</sup> Errors are reported as  $\pm \sigma$ .

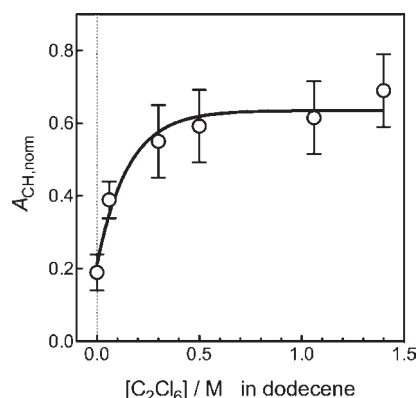


**Figure 6.** Effect of the concentration of  $\text{C}_2\text{Cl}_6$  on the amount hydrosilylation yield on PS after 90 s of white-light photolysis.

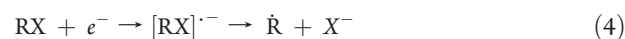
Sailor and co-workers<sup>32</sup> and our spectra are qualitatively similar (see Supporting Information).

Further support for electron transfer from the surface comes from an experiment in which a PS surface was coated with 0.5 M  $\text{C}_2\text{Cl}_6$  in hexanes and irradiated for 60 s with white light. In comparison, a sample coated with neat hexanes and irradiated for the same time period showed a higher degree of surface oxidation (see Supporting Information, Figure S6). These results are consistent with a  $h^+$  that is more susceptible to nucleophilic attack (by adventitiously formed  $\text{O}_2^-$ ) in the presence of the halocarbon oxidant.<sup>20</sup>

The rate of hydrosilylation on PS coated with dodecene, 0.5 M  $\text{CCl}_4$  in dodecene, and 0.5 M  $\text{C}_2\text{Cl}_6$  in dodecene was monitored over the course of several minutes (Figure 5). The data were fit to the first-order growth equation (eq 3),<sup>33</sup> where  $A_t$  is the normalized  $\text{CH}_x$  absorption ( $A_{\text{CH},\text{norm}}$ ) at time  $t$  and  $A_{\text{max}}$  is the maximum value of  $A_{\text{CH},\text{norm}}$  reached over the course of the experiment. The observed rate coefficients are listed in Table 2. Hydrosilylation is approximately twice as fast in the presence of  $\text{CCl}_4$  and  $\text{C}_2\text{Cl}_6$  (at 0.5 M); the maximum yield is also increased.

$$A_t = A_{\text{max}}(1 - e^{-kt}) \quad (3)$$

The yield of hydrosilylation increases with increasing concentration of  $\text{C}_2\text{Cl}_6$ , particularly over the range of 0–0.5 M  $\text{C}_2\text{Cl}_6$  (see Figure 6); above this concentration the yield is relatively constant (dodecene becomes saturated with  $\text{C}_2\text{Cl}_6$  at  $\sim 1.7 \text{ M}$ ).<sup>34</sup> Reduction of halocarbons is often dissociative, yielding an alkyl radical and halide anion (eq 4),<sup>21</sup> and thus a number of experiments were carried out to explore the possibility of a radical-based hydrosilylation



reaction.<sup>21</sup> First, the yields of hydrosilylation reactions in the presence of  $C_2Cl_6$  were not affected by the presence of the radical trap 2,6-di-*tert*-butyl-4-methylphenol (BHT) over the concentration range of 0.05–1.0 M BHT, suggesting that, if alkyl radicals are formed, they do not play a major role in the surface reaction mechanism. Second, benzyl chloride as an oxidizing agent provides a handle to determine whether the oxidant itself becomes incorporated into the surface via a Si–C bond; the lack of aromatic infrared  $CH_x$  stretching ( $>3000\text{ cm}^{-1}$ ) and bending modes ( $1400\text{--}1600\text{ cm}^{-1}$ ) indicates it does not (Figure 3e). Third, in terms of the reactivity of a silicon-based radical in a competitive situation with alkyl chlorides and alkenes, previous work by Chatgialiloglu et al. suggests that Si–Cl bond formation would be observed. This group measured the absolute rate constants for the chlorine-abstraction and addition reactions of silyl radicals with halocarbons and alkenes, respectively.<sup>35</sup> For example, the rate constants at 300 K for the reactions of  $\bullet SiEt_3$  with 1-hexene,  $CH_2Cl_2$ ,  $CHCl_3$ , and  $CCl_4$  are  $4.8 \times 10^6\text{ M}^{-1}\text{ s}^{-1}$ ,  $7.1 \times 10^7\text{ M}^{-1}\text{ s}^{-1}$ ,  $2.5 \times 10^8\text{ M}^{-1}\text{ s}^{-1}$ ,  $4.3 \times 10^9\text{ M}^{-1}\text{ s}^{-1}$ , respectively.<sup>35a,b</sup> The rate constants of the halocarbons with  $\bullet SiEt_3$  are at least an order of magnitude faster than the Si–C bond-forming reaction with the alkene. We would therefore expect at least some Si–Cl bond formation (even despite the higher concentration of the alkene) on the surface in the event that surface radicals were being formed to any great extent. In terms of direct observation of Si–Cl bonds via infrared spectroscopy, the  $\nu(Si-Cl)$  appears  $\sim 520\text{--}580\text{ cm}^{-1}$  in the fingerprint region of the spectrum,<sup>36</sup> and although this region does not appear to change significantly after reaction in the presence of halocarbons, the absence of change alone is not convincing. In the event that Si–Cl bonds were formed, they would rapidly oxidize upon exposure to air, leading to an increase in the intensity of the Si–O absorbance by FTIR,<sup>37</sup> which is not observed. Finally, oxidation of the silicon (as determined by the Si 2p signal) in X-ray photoelectron spectroscopy (XPS) is also not observed.

XPS of the PS surfaces after hydrosilylation with 0.5 M  $C_2Cl_6$  in dodecene shows, however, the presence of chlorine (see Supporting Information, Figure S7). No chlorine signal was observed on a dark control sample that was exposed to 0.5 M  $C_2Cl_6$  in dodecene for 10 min in the dark and then rinsed with DCM. A ToF-SIMS depth profile of a similar sample shows the intensity of the chlorine signal is less than but tracks that of carbon (see Supporting Information, Figure S8b), suggesting either that the chlorine is attached to an alkyl chain or that the alkyl chains attached to the PS assist in the getting of the halocarbon. To test the latter possibility, a sample of PS underwent exciton-mediated hydrosilylation with neat dodecene and was then coated with a solution of 0.5 M  $C_2Cl_6$  in dodecene and kept in the dark for 5 min; the sample was rinsed twice with DCM prior to analysis. ToF-SIMS depth analysis of this sample also showed a strong chlorine signal and that the chlorine intensity tracked that of carbon (see Supporting Information, Figure S8c). These surface analyses suggest the source of chlorine is likely adsorbed halocarbon rather than chlorine chemically bonded to the alkyl chains or the PS surface.

In order to chemically demonstrate the central role of the exciton in the hydrosilylation mechanism, a molecule known to quench the exciton and halt the hydrosilylation reaction was employed.<sup>5</sup> Ferrocene ( $E_{ox} = +0.66\text{ V vs SHE}$ )<sup>38</sup> will quench the exciton through donation of an electron to the surface<sup>39</sup> and suppress the white-light mediated hydrosilylation reaction on PS through this charge-transfer mechanism. Ferrocene was added at

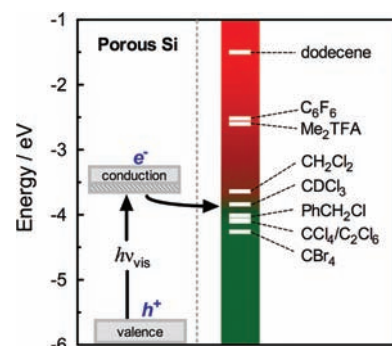


**Figure 7.** Energy level diagram showing the valence and conduction bands of PS and the LUMOs of select oxidizing agents. PS valence and conduction band energies from reference 18e; the shaded region is the lower limit of the conduction band energy based on these experiments. LUMO energies of the oxidizing agents are based on the reduction potentials in Table 1.

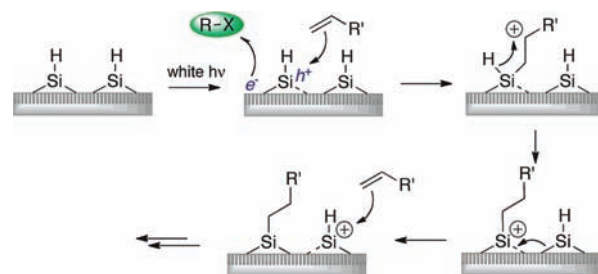


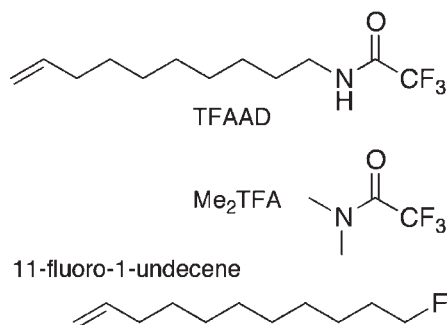
**Figure 8.** Proposed mechanism for the exciton-mediated PS hydrosilylation facilitated by the presence of a halocarbon (RX).  $R' = n-C_{10}H_{21}$ .

concentrations of 14 mM and 25 mM to solutions of 0.5 M  $C_2Cl_6$  in dodecene, and the photolysis experiments were carried out in the usual manner. In the presence of 14 mM and 25 mM ferrocene, the yield of hydrosilylation decreases by a factor of 2–3 relative to the yield obtained in the absence of ferrocene (see Supporting Information, Figure S9), thus supporting an exciton-driven mechanism.

Electron extraction and transfer from the exciton of PS to the LUMO of the oxidizing agent is shown in Figure 7. While such a representation is an oversimplification of the range of band energies of the morphologically complex PS, the energy of the PS conduction band as determined from the “turn on” potentials using the oxidizing agents in this study ( $\sim -3.6 \pm 0.2\text{ eV}$ ) is in good agreement with the value reported by Rehm et al. ( $-3.3 \pm 0.2\text{ eV}$ ).<sup>18e</sup> Upon generation of the exciton, the electron can only be transferred to those molecules with a LUMO energy below that of the PS conduction band; only in these cases can the exciton-binding energy be overcome. The exciton-binding energy is a result of the Coulombic attraction between  $e^-$  and  $h^+$  and for porous silicon with its distribution of nanocrystallite sizes, it ranges from a predicted 1.4 to 0.15 eV in silicon nanocrystallites of radius 0.4 to 2 nm, respectively.<sup>40</sup> As the LUMO energy of the acceptor decreases, it is able to accept the electron from a larger fraction of the PS excitons, in turn generating more positive charges on the surface. The positively charged surface ( $h^+$ ) is susceptible to attack by the  $\pi$  electrons of the alkene, as shown schematically in Figure 8. The initial attack presumably

leads to a  $\beta$ -silyl cation, followed by a hydride transfer from the silicon to the alkyl chain. Migration of the positive charge along the surface allows for additional hydrosilylation reactions, analogous to what has been proposed for hydride abstraction-initiated PS hydrosilylation.<sup>4e</sup>

At this point, we considered whether sacrificial electron acceptors might also be effective at increasing the yield of UV-initiated hydrosilylation of hydrogen-terminated flat silicon. In their recent study of UV-initiated hydrosilylation on hydrogen-terminated flat silicon<sup>3</sup> and the grafting of alkenes onto hydrogen-terminated carbon,<sup>41</sup> Hamers and co-workers employed several terminal alkenes with different valence orbital energies and in each case found that surfaces coated with the alkene *N*-(dec-9-enyl)-trifluoroacetamide (TFAAD) gave the highest reaction yield. Of the alkenes studied, TFAAD has the greatest electron affinity.



UV photons (254 nm) have sufficient energy to eject an electron from the surface and it was rationalized that TFAAD most readily captured the electron. Once the electron is captured, a positive hole ( $h^+$ ) remains on the surface, which is then attacked by the alkene (see Figure 1 *ii*). In principle, many of the halocarbons used as oxidizing agents in the PS experiments should also result in an increased yield of UV-initiated hydrosilylation on Si(111)–H because they possess greater reduction potentials than TFAAD. While the electron affinity is an enthalpic term measured in the gas phase and the reduction potential is a Gibbs energy term measured in solution,<sup>42</sup> the two generally track together.<sup>43</sup> Based on their reduction potentials, CH<sub>2</sub>Cl<sub>2</sub> and CHCl<sub>3</sub> should also be effective at trapping an ejected electron. These are also transparent at high concentrations to 254 nm light (see Supporting Information, Figure S10). An additional consideration is that UV irradiation of the silicon surface is generally believed to lead to the formation of radicals and there would be a competition between the alkene and the halocarbon for reaction with the radical (*vide supra*). Despite this possible complication, we opted to investigate whether the presence of these halocarbons would increase the yield of hydrosilylation of Si(111)–H. We also used Me<sub>2</sub>TFA because, on the basis of the work of Hamers and co-workers with TFAAD,<sup>3</sup> it should lead to an increased yield of hydrosilylation. The amide functional group of TFAAD accepts the electron, and thus Me<sub>2</sub>TFA should be a reasonable model for TFAAD; the additional *N*-methyl should result in only a minor decrease in the electron affinity.<sup>44</sup>

11-Fluoro-1-undecene was used for flat silicon hydrosilylation in order to allow the relative degree of grafting to be estimated by the intensity of the F 1s signal by XPS. In an inert atmosphere, Si(111)–H was coated with a small volume of the neat alkene or alkene containing 1 M of the electron acceptor and irradiated with 254 nm light. Samples were soaked twice in dichloromethane, removed from the glovebox, and immediately analyzed

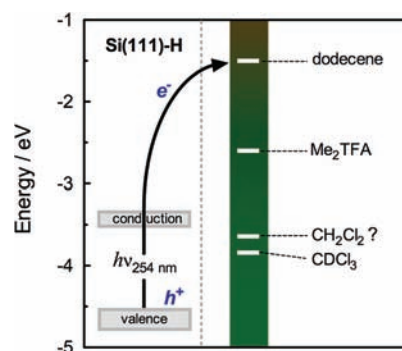


**Figure 9.** Energy level diagram showing the photoejection of an electron from Si(111)–H and the LUMOs of the electron acceptors. Si(111)–H valence and conduction band energies taken from reference 46.

by XPS. In the presence of Me<sub>2</sub>TFA, the yield of hydrosilylation was  $\sim 2.5$  times greater than with the neat alkene (see Supporting Information, Figure S11), which is in agreement with Hamers and co-workers.<sup>3</sup> Chloroform also resulted in an increased yield ( $\sim 2$  times greater), but dichloromethane did not. We were conscious of the volatility of dichloromethane, which prompted us to attempt an alternate method in which the alkene/halocarbon mixtures were sealed directly onto the silicon surface with a quartz slide. Although we cannot entirely rule out evaporation of the solvent, the fact that CH<sub>2</sub>Cl<sub>2</sub> did not lead to a greater yield was surprising, given the reduction potentials. Figure 9 shows an energy level diagram relevant to the experiments on Si(111)–H. In principle, because the energy of the photoejected electron exceeds that of the LUMOs of dodecene and all the halocarbons employed in these experiments, all should act as effective electron acceptors. On the basis of the LUMO energies, any of the halocarbons added to the solution should more be more efficient at capturing the electron than dodecene. It is therefore reasonable that both Me<sub>2</sub>TFA and CDCl<sub>3</sub> resulted in an increased yield of hydrosilylation. XPS analyses of the surface did *not* indicate the presence of chlorine (either through the 2s or 2p signals), nor was oxidation of the silicon surface (based on the Si 2p spectra) observed.<sup>45</sup> Experiments to further our understanding of these preliminary experiments on Si(111)–H are ongoing, but our results nevertheless indicate that sacrificial electron acceptors dissolved in the alkene result in an increased yield of hydrosilylation of flat surfaces as well as with porous silicon.

In summary, these results show that in the presence of halocarbons with high reduction potentials ( $E_{\text{red}} > -0.6$  V in acetonitrile vs SHE), the rate and yield of PS exciton-mediated hydrosilylation are increased without accompanying surface oxidation. The proposed mechanism involves initial reduction of the halocarbon by the exciton electron, followed by attack of  $h^+$  by the alkene. Because the electron has been removed,  $h^+$  can migrate along the surface, allowing further reaction. This not only provides a method of increasing the yield of surface functionalization but also more importantly provides insight into the mechanism of exciton-mediated hydrosilylation and the nature of the excited state of PS. Preliminary results suggest that a similar phenomenon may take place in the presence of halocarbons with UV-initiated flat silicon, in agreement with the experiments of Hamers and co-workers.<sup>3</sup> Although the experiments with PS and Si(111)–H are similar in that the presence of an electron acceptor increases the yield of hydrosilylation, the difference is that the PS requires a much stronger oxidizing agent because the

exciton binding energy<sup>10</sup> must be overcome in order for the loss of the electron to take place; with Si(111)–H, the binding energy (which is much less than that of PS)<sup>47</sup> is overcome by absorption of the higher energy photon and ejection of the electron. We are currently expanding our experiments to other alkenes and alkynes on PS and flat silicon, exploring the stability of the resulting alkyl monolayers prepared by these methods as well as the general phenomenon of electron transfer from the PS surface.

## CONCLUSIONS

The yield and rate of white-light initiated hydrosilylation on PS increase dramatically in the presence of halocarbons with reduction potentials  $E_{\text{red}} > -0.6 \text{ V}$  (vs  $\text{SHE}_{\text{MeCN}}$ ). This observed increase in reaction efficiency is due to the ability of the halocarbon to oxidize the exciton, rendering the positively charged silicon nanoparticle more susceptible to attack by the alkene. In a photoemission-based mechanism with UV irradiation ( $\lambda = 254 \text{ nm} = 4.9 \text{ eV}$ ) on Si(111)–H surfaces, the photon energy exceeds the work function of the surface and thus leads directly to photoemission and ejection of the electron (leaving a positive charge on the surface to react). In the white-light exciton-based mechanism, on the other hand ( $\lambda_{\text{min}} = 400 \text{ nm} = 3.1 \text{ eV}$ ) in a silicon nanocrystallite, a stronger oxidizing agent is required to remove the electron from the exciton to overcome the exciton binding energy. Understanding and controlling charge transfer from excitons is a key challenge for device function, and to further harness their chemical reactivity;<sup>10b,48</sup> these results provide insight into exciton charge transfer on silicon nanocrystallites.

## EXPERIMENTAL SECTION

**Equipment.** White light used for the preparation of PS and the hydrosilylation reaction was generated using a 500 W halogen work light and a 300 W ELH projector bulb, respectively. Light intensity was measured with a Metrologic Radiometer. The current used in the PS synthesis was controlled with an EG&G Princeton Applied Research potentiostat–galvanostat model 363. FTIR spectra were collected with a Nicolet Nexus 760 spectrometer with a DTGS detector and a  $\text{N}_2$ -purged sample chamber (32 scans,  $4 \text{ cm}^{-1}$  resolution); the area of the SiH and CH signals were taken over  $2000\text{--}2200 \text{ cm}^{-1}$  and  $2800\text{--}3050 \text{ cm}^{-1}$ , respectively. Scanning electron microscopy (SEM) images were obtained with a Hitachi S-4800 FE-SEM ( $P < 10^{-8}$  Torr) with an accelerating voltage of 15 kV. X-ray photoelectron spectroscopy (XPS) data were obtained on a Kratos Axis 165 X-ray photoelectron spectrometer ( $P < 10^{-8}$  Torr) using a monochromatic Al  $K\alpha$  with a photon energy of 1486.6 eV; ejected electrons were measured at  $0^\circ$  from the surface normal. The XPS signals were calibrated using the C(1s) signal (284.8 eV). ToF-SIMS analysis was carried out with an ION-ToF (GmbH) 100 instrument. The dual-beam profiling mode was used sputtering with a rastered  $\text{Cs}^+$  source at 1 keV led to a crater size of  $200 \mu\text{m} \times 200 \mu\text{m}$ , with analysis by  $\text{Ga}^+$  at 25 keV,  $30.3 \mu\text{m} \times 30.3 \mu\text{m}$ . UV light (254 nm) for Si(111)–H experiments was supplied by a UVP pen-lamp ( $\sim 4 \text{ mW cm}^{-2}$  with the lamp 2 cm above the sample).

**Materials.** Silicon wafers (prime-grade, *n*-type, P-doped, 1–3  $\Omega\text{cm}$ , 450–500  $\mu\text{m}$ ) were obtained from Virginia Semiconductor Inc. Acetone (Fisher, reagent), carbon tetrabromide (Aldrich, 99%), ethanol (Fisher, absolute), ferrocene (Aldrich, 98%), HF (49%, J. T. Baker), hexachloroethane (Aldrich, 99%), pentane (Fisher, reagent), and alumina (Aldrich, Brockmann Neutral I) were used as received. Benzyl chloride (Aldrich, 99%), carbon tetrachloride (Aldrich, >99.9%), chloroform-*d* (Aldrich, >99%), 1-dodecene (Aldrich, >95%), hexafluorobenzene (Aldrich, 99%) were

passed as neat liquids through a column of alumina, sealed in a flask, and deoxygenated with a fine stream of argon for at least 30 min. Dichloromethane and hexanes were obtained from a solvent purification system (Innovative Technologies, Inc.). 11-Fluoro-1-undecene was prepared following a literature procedure<sup>2f</sup> and passed as a neat liquid through alumina prior to use. *N,N*-dimethyltrifluoroacetamide (Oakwood Chemicals, >97%) was passed as a neat liquid through a column of silica, a column of alumina, sealed in a flask, and deoxygenated with a fine stream of argon for at least 30 min.

**Preparation of Porous Silicon.** Silicon wafers were cut into  $1 \text{ cm}^2$  pieces, sonicated in 1:1 acetone:ethanol for 10 min, rinsed with ethanol, and dried with argon gas. PS was prepared following a literature procedure,<sup>5</sup> which is described briefly. Using 1:1 49% HF:EtOH as the electrolyte/etchant, the silicon was anodized at  $7.6 \text{ mA cm}^{-2}$  for 90 s and then  $76 \text{ mA cm}^{-2}$  for 120 s with full white-light illumination ( $\sim 40 \text{ mW cm}^{-2}$ ).<sup>49</sup> The sample was rinsed with ethanol (but not allowed to dry), immersed in pentane, and dried with and stored under argon in the dark. This method produces photoluminescent PS, which was confirmed using a hand-held 365-nm lamp. SEM images of the PS are shown in the Supporting Information Figure S1. Infrared spectra were recorded of each sample before and after photolysis.

**Exciton-Mediated Hydrosilylation.** All PS photolysis experiments were performed within an inert atmosphere glovebox. Each wafer was coated with  $40 \mu\text{L}$  of the alkene or alkene/oxidant solution. White light was focused on the sample using a PCX lens. Infrared filters were placed above the lens and between the lens and the sample. (The absorbance spectra of these filters are given in the Supporting Information, Figure S2.) After photolysis, the wafers were soaked in dichloromethane within the glovebox to remove most of the organics. The samples were then removed from the glovebox, rinsed again with dichloromethane, and dried with argon gas prior to analysis.

**Preparation and Functionalization of Si(111)–H.** Si(111) *n*-type, P doped (1–5 W cm;  $381 \pm 25 \text{ mm}$  thick) wafers were cut into  $1 \text{ cm}^2$  pieces and cleaned using the standard RCA procedure.<sup>50</sup> The wafers were immersed in argon-saturated, aqueous  $\text{NH}_4\text{F}$  (40%) for four minutes, dipped in deionized water for 5 s ( $\times 2$ ), and dried with a stream of argon gas. All photolyses were performed within an inert atmosphere glovebox. Samples of Si(111)–H were placed either (a) within a Teflon sample holder (which allows a 7 mm diameter area to be exposed to the light), coated with  $30 \mu\text{L}$  of the neat alkene or alkene/electron acceptor [The sample holder was sealed with a quartz slide. There is about 8 mm of headspace between the sample and quartz slide. Samples were irradiated for 30 min.] or (b) on a glass slide, coated with a  $30 \mu\text{L}$  of the neat alkene or alkene/electron acceptor, covered with a quartz slide placed directly on top of the surface. Samples were irradiated for 2 min. This method allowed a much higher intensity of light to reach the surface and was also used to prevent evaporation of the electron acceptor from the alkene. In each case, samples were soaked in DCM, removed from the glovebox, rinsed again with DCM, dried with a stream of argon, and immediately analyzed by XPS.

## ASSOCIATED CONTENT

**Supporting Information.** SEM images of the photoluminescent PS; absorption spectra of UV and IR filters; UV spectra of  $\text{CDCl}_3$ ,  $\text{C}_2\text{Cl}_6$ ,  $\text{PhCH}_2\text{Cl}$ ,  $\text{CBr}_4$ , and  $\text{Me}_2\text{TFA}$ ; XPS and ToF-SIMS depth profiles of the PS and Si(111), analysis details. This material is available free of charge via the Internet at <http://pubs.acs.org>.

## AUTHOR INFORMATION

### Corresponding Author

lhuck@ualberta.ca; jburiaak@ualberta.ca

## ACKNOWLEDGMENT

We thank the Natural Sciences and Engineering Research Council (NSERC) of Canada, the National Research Council (NRC), Canada–National Institute for Nanotechnology (NINT), the Canadian Foundation for Innovation (CFI), and the University of Alberta. L.A.H. thanks NSERC for a postdoctoral fellowship. We also thank the Alberta Center for Surface Engineering and Science (ACES) for XPS and ToF-SIMS analyses.

## REFERENCES

- (1) (a) *Handbook of Semiconductor Technology*; Wiley-VCH: Weinheim, 2000; Vol. 2. (b) Ashkenasy, G.; Cahen, D.; Cohen, R.; Shanzer, A.; Vilan, A. *Acc. Chem. Res.* **2002**, *35*, 121. (c) Bent, S. F. *Surf. Sci.* **2002**, *500*, 879. (d) Campbell, S. A. *Fabrication Engineering at the Micro- and Nanoscale*, 3rd ed.; Oxford: New York, 2008. (e) Leftwich, T. R.; Teplyakov, A. V. *Surf. Sci. Rep.* **2008**, *63*, 1. (f) Kachian, J. S.; Wong, K. T.; Bent, S. F. *Acc. Chem. Res.* **2010**, *43*, 346. (g) Yates, J. T., Jr.; Campbell, C. T. *Proc. Natl. Acad. Sci. U.S.A.* **2011**, *108*, 911.
- (2) (a) Linford, M. R.; Fenter, P.; Eisenberger, P. M.; Chidsey, C. E. D. *J. Am. Chem. Soc.* **1995**, *117*, 3145. (b) Boukherroub, R.; Morin, S.; Bensebaa, F.; Wayner, D. D. M. *Langmuir* **1999**, *15*, 3831. (c) Cicero, R. L.; Linford, M. R.; Chidsey, C. E. D. *Langmuir* **2000**, *16*, 5688. (d) de Smet, L. C. P. M.; Zuilhof, H.; Sudhölter, E. J. R.; Lie, L. H.; Houlton, A.; Horrocks, B. R. *J. Phys. Chem. B* **2005**, *109*, 12020. (e) Langer, A.; Panarello, A.; Rivillon, S.; Vassilyev, O.; Khinast, J. G.; Chabal, Y. J. *J. Am. Chem. Soc.* **2005**, *127*, 12798. (f) Sun, Q.-Y.; de Smet, L. C. P. M.; van Lagen, B.; Giesbers, M.; Thüne, P. C.; van Engelenburg, J.; de Wolf, F. A.; Zuilhof, H.; Sudhölter, E. J. R. *J. Am. Chem. Soc.* **2005**, *127*, 2514. (g) Eves, B. J.; Lopinski, G. P. *Langmuir* **2006**, *22*, 3180. (h) Scheres, L.; Arafat, A.; Zuilhof, H. *Langmuir* **2007**, *23*, 8343. (i) Scheres, L.; Giesbers, M.; Zuilhof, H. *Langmuir* **2010**, *26*, 10924. (j) Scheres, L.; Giesbers, M.; Zuilhof, H. *Langmuir* **2010**, *26*, 4790. (k) Zhong, Y. L.; Bernasek, S. L. *Langmuir* **2011**, *27*, 1796. (l) Zhong, Y. L.; Bernasek, S. L. *J. Am. Chem. Soc.* **2011**, *133*, 8118. (m) Bansal, A.; Li, X.; Lauermann, I.; Lewis, N. S.; Yi, S. I.; Weinberg, W. H. *J. Am. Chem. Soc.* **1996**, *118*, 7225. (n) de Villeneuve, C. H.; Pinson, J.; Bernard, M. C.; Allongue, P. *J. Phys. Chem. B* **1997**, *101*, 2415. (o) Gurtner, C.; Wun, A. W.; Sailor, M. J. *Angew. Chem., Int. Ed.* **1999**, *38*, 1966. (p) Buriak, J. M. *Chem. Rev.* **2002**, *102*, 1271. (q) Wayner, D. D. M.; Wolkow, R. A. *J. Chem. Soc., Perkin Trans. 2* **2002**, 23. (r) Filler, M. A.; Bent, S. F. *Prog. Surf. Sci.* **2003**, *73*, 1. (s) Stewart, M. P.; Maya, F.; Kosynkin, D. V.; Dirk, S. M.; Stapleton, J. J.; McGuinness, C. L.; Allara, D. L.; Tour, J. M. *J. Am. Chem. Soc.* **2004**, *126*, 370. (t) Pinson, J.; Podvorica, F. *Chem. Soc. Rev.* **2005**, *34*, 429. (u) Hamers, R. J. *Annu. Rev. Anal. Chem.* **2008**, *1*, 707. (v) Ciampi, S.; Harper, J. B.; Gooding, J. J. *Chem. Soc. Rev.* **2010**, *39*, 2158.
- (3) Wang, X.; Ruther, R. E.; Streifer, J. A.; Hamers, R. J. *J. Am. Chem. Soc.* **2010**, *132*, 4048.
- (4) (a) Stewart, M. P.; Buriak, J. M. *Angew. Chem., Int. Ed.* **1998**, *37*, 3257. (b) Buriak, J. M.; Stewart, M. P.; Geders, T. W.; Allen, M. J.; Choi, H. C.; Smith, J.; Raftery, D.; Canham, L. T. *J. Am. Chem. Soc.* **1999**, *121*, 11491. (c) Bateman, J. E.; Eagling, R. D.; Horrocks, B. R.; Houlton, A. *J. Phys. Chem. B* **2000**, *104*, 5557. (d) Boukherroub, R.; Morin, S.; Wayner, D. D. M.; Bensebaa, F.; Sproule, G. I.; Baribeau, J.-M.; Lockwood, D. J. *Chem. Mater.* **2001**, *13*, 2002. (e) Schmeltzer, J. M.; Porter, L. A., Jr.; Stewart, M. P.; Buriak, J. M. *Langmuir* **2002**, *18*, 2971. (f) Boukherroub, R.; Petit, A.; Loupy, A.; Chazalviel, J.-N.; Ozanam, F. *J. Phys. Chem. B* **2003**, *107*, 13459. (g) Li, Y.-H.; Buriak, J. M. *Inorg. Chem.* **2006**, *45*, 1096. (h) Petit, A.; Delmotte, M.; Loupy, A.; Chazalviel, J.-N.; Ozanam, F.; Boukherroub, R. *J. Phys. Chem. C* **2008**, *112*, 16622. (i) Kelly, J. A.; Shukaliak, A. M.; Fleischauer, M. D.; Veinot, J. G. C. *J. Am. Chem. Soc.* **2011**, *133*, 9564. (j) Jariwala, B. N.; Dewey, O. S.; Stradins, P.; Ciobanu, C. V.; Agarwal, S. *ACS Appl. Mater. Interfaces* **2011**, *3*, 3033. (k) Bateman, J. E.; Eagling, R. D.; Worrall, D. R.; Horrocks, B. R.; Houlton, A. *Angew. Chem., Int. Ed.* **1998**, *37*, 2683. (l) Kim, N. Y.; Laibinis, P. E. *J. Am. Chem. Soc.* **1998**, *120*, 4516. (m) Song, J. H.; Sailor, M. J. *J. Am. Chem. Soc.* **1998**, *120*, 2376. (n) Buriak, J. M. *Chem. Commun.* **1999**, 1051. (o) Song, J. H.; Sailor, M. J. *Comments Inorg. Chem.* **1999**, *21*, 69. (p) Stewart, M. P.; Buriak, J. M. *Comments Inorg. Chem.* **2002**, *23*, 179. (q) Schwartz, M. P.; Cunin, F.; Cheung, R. W.; Sailor, M. J. *Phys. Status Solidi A* **2005**, *202*, 1380. (r) Wang, D.; Buriak, J. M. *Surf. Sci.* **2005**, *590*, 154. (s) Veinot, J. G. C. *Chem. Commun.* **2006**, 4160. (t) *Silicon Nanocrystals: Fundamentals, Synthesis and Applications*; Wiley-VCH: Weinheim, 2010.
- (5) Stewart, M. P.; Buriak, J. M. *J. Am. Chem. Soc.* **2001**, *123*, 7821.
- (6) (a) Linford, M. R.; Chidsey, C. E. D. *J. Am. Chem. Soc.* **1993**, *115*, 12631. (b) Sun, Q.-Y.; de Smet, L. C. P. M.; van Lagen, B.; Wright, A.; Zuilhof, H.; Sudhölter, E. J. R. *Angew. Chem., Int. Ed.* **2004**, *43*, 1352. (c) Boukherroub, R. *Curr. Opin. Solid State Mater. Sci.* **2005**, *9*, 66. (d) Buriak, J. M.; Allen, M. J. *J. Am. Chem. Soc.* **1998**, *120*, 1339.
- (7) (a) Wagner, P.; Nock, S.; Spudich, J. A.; Volkmuth, W. D.; Chu, S.; Cicero, R. L.; Wade, C. P.; Linford, M. R.; Chidsey, C. E. D. *J. Struct. Biol.* **1997**, *119*, 189. (b) Terry, J.; Mo, R.; Wigren, C.; Cao, R.; Mount, G.; Pianetta, P.; Linford, M. R.; Chidsey, C. E. D. *Nucl. Instrum. Methods Phys. Res.* **1997**, *133*, 94. (c) Effenberger, F.; Götz, G.; Bidlingmaier, B.; Wezstein, M. *Angew. Chem., Int. Ed.* **1998**, *37*, 2462.
- (8) Eves, B. J.; Sun, Q.-Y.; Lopinski, G.; Zuilhof, H. *J. Am. Chem. Soc.* **2004**, *126*, 14318.
- (9) Kanai, Y.; Selloni, A. *J. Am. Chem. Soc.* **2006**, *128*, 3892.
- (10) (a) Nirmal, M.; Brus, L. *Acc. Chem. Res.* **1999**, *32*, 407. (b) Heitmann, J.; Müller, F.; Yi, L.; Zacharias, M.; Kovalev, D.; Eichhorn, F. *Phys. Rev. B* **2004**, *69*, 195309.
- (11) Canham, L. T. *Appl. Phys. Lett.* **1990**, *57*, 1046.
- (12) Canham, L., Ed. *Properties of Porous Silicon*; INSPEC, Institute of Electrical Engineers: London, 1997.
- (13) (a) Salonen, J.; Kaukonen, A. M.; Hirvonen, J.; Lehto, V.-P. *J. Pharm. Sci.* **2008**, *97*, 632. (b) Anglin, E. J.; Cheng, L.; Freeman, W. R.; Sailor, M. J. *Adv. Drug Delivery Rev.* **2008**, *60*, 1266.
- (14) (a) Jane, A.; Dronov, R.; Hodges, A.; Voelcker, N. H. *Trends Biotechnol.* **2009**, *27*, 230. (b) Singh, P.; Sharma, S. N.; Ravindra, N. M. *JOM* **2010**, *62*, 15. (c) Salonen, J.; Lehto, V.-P. *Chem. Eng. J.* **2008**, *137*, 162. (d) Fan, J.; Chu, P. K. *Small* **2010**, *6*, 2080.
- (15) (a) Yerokhov, V. Y.; Melnyk, I. I. *Renewable Sustainable Energy Rev.* **1999**, *3*, 291. (b) Parida, B.; Iniyani, S.; Goic, R. *Renewable Sustainable Energy Rev.* **2011**, *15*, 1625.
- (16) Boukherroub, R. *Device Applications of Silicon Nanocrystals and Nanostructures*; Springer: New York, 2009.
- (17) Romstad, F. P.; Veje, E. *Phys. Rev. B* **1997**, *55*, 5220.
- (18) (a) Buda, F.; Kohanoff, J.; Parrinello, M. *Phys. Rev. Lett.* **1992**, *69*, 1272. (b) Canham, L. T. *Applied Sciences - Optical Properties of Low Dimensional Silicon Structures*. In *NATO Advanced Study Institute Series E244*; Bensahel, D. C., Canham, L. T., Ossicini, S., Eds.; Kluwer: Dordrecht, 1993; p 81. (c) Fisher, D. L.; Gamboa, A.; Harper, J.; Lauerhaas, J. M.; Sailor, M. J. *Mater. Res. Soc. Symp. Proc.* **1995**, *358*, 507. (d) Coffer, J. L. *J. Lumin.* **1996**, *70*, 343. (e) Rehm, J. M.; McLendon, G. L.; Fauchet, P. M. *J. Am. Chem. Soc.* **1996**, *118*, 4490. (f) Baierle, R. J.; Caldas, M. J.; Molinari, E.; Ossicini, S. *Solid State Commun.* **1997**, *102*, 545. (g) Cullis, A. G.; Canham, L. T.; Calcott, P. D. *J. Appl. Phys.* **1997**, *82*, 909.
- (19) Heinrich, J. L.; Lee, A.; Sailor, M. J. *Mater. Res. Soc. Symp. Proc.* **1995**, *358*, 605.
- (20) Harper, J.; Sailor, M. J. *Langmuir* **1997**, *13*, 4652.
- (21) (a) Savéant, J.-M. *Adv. Phys. Org. Chem.* **2000**, *35*, 117. (b) Houmam, A. *Chem. Rev.* **2008**, *108*, 2180.
- (22) Stewart, M. P.; Robins, E. G.; Geders, T. W.; Allen, M. J.; Choi, H. C.; Buriak, J. M. *Phys. Status Solidi A* **2000**, *182*, 109.
- (23) Scheres, L.; Rijksen, B.; Giesbers, M.; Zuilhof, H. *Langmuir* **2011**, *27*, 972.
- (24) Isse, A. A.; Lin, C. Y.; Coote, M. L.; Gennaro, A. *J. Phys. Chem. B* **2011**, *115*, 678.
- (25) Kariv-Miller, E.; Pacut, R. I.; Lehman, G. K. *Top. Curr. Chem.* **1988**, *148*, 97.
- (26) Magdesieva, T. V.; Shishkin, V. N.; Butin, K. P. *Zh. Obshch. Khim. (Eng. Transl.)* **1991**, *61*, 2403.

- (27) Spahr, M. E.; Palladino, T.; Wilhelm, H.; Würsig, A.; Goers, D.; Buqa, H.; Holzapfel, M.; Novák, P. *J. Electrochem. Soc.* **2004**, *151*, A1383.
- (28) Gritzner, G. *J. Phys. Chem.* **1986**, *90*, 5478.
- (29) Totten, L. A.; Roberts, A. L. *Crit. Rev. Env. Sci. Technol.* **2001**, *31*, 175.
- (30) Berionni, G.; Gonçalves, A.-M.; Mathieu, C.; Devic, T.; Etchéberry, A.; Goumont, R. *Phys. Chem. Chem. Phys.* **2011**, *13*, 2857.
- (31) Germanenko, I. N.; Li, S.; El-Shall, M. S. *J. Phys. Chem. B* **2001**, *105*, 59.
- (32) Content, S.; Trogler, W. C.; Sailor, M. J. *Chem.—Eur. J.* **2000**, *6*, 2205.
- (33) Espenson, J. H. *Chemical Kinetics and Reaction Mechanisms*, 2nd ed.; McGraw-Hill Book Co.: New York, 1995; pp 15–18.
- (34) Compared with  $\text{CCl}_4$ ,  $\text{C}_2\text{Cl}_6$  has a number of practical advantages: it is a solid and easy to handle, available in small amounts, relatively inexpensive, and not restricted as an ozone-depleting substance. For these reasons, most of our experiments were performed with this halocarbon.
- (35) (a) Chatgililoglu, C.; Ingold, K. U.; Scaiano, J. C. *J. Am. Chem. Soc.* **1982**, *104*, 5123. (b) Chatgililoglu, C.; Ingold, K. U.; Scaiano, J. C. *J. Am. Chem. Soc.* **1983**, *105*, 3292. (c) Chatgililoglu, C.; Griller, D.; Lesage, M. *J. Org. Chem.* **1989**, *54*, 2492.
- (36) Webb, L. J.; Rivillon, S.; Michalak, D. J.; Chabal, Y. J.; Lewis, N. S. *J. Phys. Chem. B* **2006**, *110*, 7349.
- (37) Gresback, R.; Nozaki, T.; Okazaki, K. *Nanotechnology* **2011**, *22*, 305605.
- (38) Pavlishchuk, V. V.; Addison, A. W. *Inorg. Chim. Acta* **2000**, *298*, 97.
- (39) Lauerhaas, J. M.; Credo, G. M.; Heinrich, J. L.; Sailor, M. J. *Mater. Res. Soc. Symp. Proc.* **1992**, *256*, 137.
- (40) Allan, G.; Delerue, C.; Lannoo, M.; Martin, E. *Phys. Rev. B* **1995**, *52*, 11982.
- (41) (a) Colavita, P. E.; Sun, B.; Tse, K.-Y.; Hamers, R. J. *J. Am. Chem. Soc.* **2007**, *129*, 13554. (b) Colavita, P. E.; Streifer, J. A.; Sun, B.; Wang, X.; Warf, P.; Hamers, R. J. *J. Phys. Chem. C* **2008**, *112*, 5102. (c) Wang, X.; Colavita, P. E.; Streifer, J. A.; Butler, J. E.; Hamers, R. J. *J. Phys. Chem. C* **2010**, *114*, 4067.
- (42) Atkins, P.; de Paula, J. *Physical Chemistry*, 7th ed.; W.H. Freeman: New York, 2002; pp 267, 391.
- (43) Shalev, H.; Evans, D. H. *J. Am. Chem. Soc.* **1989**, *111*, 2667.
- (44) Desfrancois, C.; Périquet, V.; Carles, S.; Schermann, J. P.; Smith, D. M. A.; Adamowicz, L. *J. Chem. Phys.* **1999**, *110*, 4309.
- (45) Webb, L. J.; Michalak, D. J.; Biteen, J. S.; Brunschwig, B. S.; Chan, A. S. Y.; Knapp, D. W.; Meyer, H. M., III; Nemanick, E. J.; Traub, M. C.; Lewis, N. S. *J. Phys. Chem. B* **2006**, *110*, 23450.
- (46) Nakamura, T.; Miyajima, K.; Hirata, N.; Matsumoto, T.; Morikawa, Y.; Tada, H.; Nakajima, A. *Appl. Phys. A: Mater. Sci. Process.* **2010**, *98*, 735.
- (47) Burr, T. A.; Seraphin, A. A.; Werwa, E.; Kolenbrander, K. D. *Phys. Rev. B* **1997**, *56*, 4818.
- (48) (a) Shirota, Y.; Kageyama, H. *Chem. Rev.* **2007**, *107*, 953. (b) Zhu, X.-Y.; Yang, Q.; Muntwiler, M. *Acc. Chem. Res.* **2009**, *42*, 1779. (c) Hochbaum, A. I.; Yang, P. *Chem. Rev.* **2010**, *110*, 527.
- (49) (a) Zhang, X. G. *J. Electrochem. Soc.* **1991**, *138*, 3750. (b) Zhang, X. G. *J. Electrochem. Soc.* **2004**, *151*, C69.
- (50) Kern, W. In *Handbook of Silicon Wafer Cleaning Technology*, 2nd ed.; Reinhardt, K. A., Kern, W., Eds.; William Andrew Publishing: Norwich, NY, 2008; p 3.